

INELASTIC TUNNEL EFFECTS WITH EMISSION OF PHONONS IN JUNCTIONS  
OF TIN, LEAD, and INDIUM

I. K. YANSON

Physicotechnical Institute of Low Temperatures, Ukrainian Academy of Sciences

Submitted November 3, 1970

Zh. Eksp. Teor. Fiz. 60, 1759-1772 (May, 1971)

Singularities were observed on the  $d^2I/dV^2$  characteristics of Sn-SnO<sub>2</sub>-Sn, Pb-PbO-Pb, and In-InO-In tunnel junctions and are interpreted as inelastic tunneling of the electrons with phonon emission. A fine structure of the band of optical phonons was observed in the oxides PbO and SnO<sub>2</sub>. A comparison of the tunnel spectrum with the infrared spectrum of lead monoxide is made for PbO. The selection rules are discussed for excitations produced by the inelastic tunneling effect, and also the influence of the structure of the oxide on the characteristics of the tunnel spectrum.

I. INTRODUCTION

INVESTIGATIONS of the elastic tunnel effect in superconductors,<sup>[1,2]</sup> semimetals,<sup>[3]</sup> and semiconductors<sup>[4]</sup> give detailed information concerning the dependence of the density of the electronic states on the energy. However, besides the direct passage of the electrons through the potential barrier with energy conservation (Fig. 1a), inelastic tunneling processes are also possible. In these, part of the electron energy is transferred to the excitation produced either in the barrier layer itself or in the immediate vicinity of this layer (Figs. 1b-d). The inelastic tunnel effect was initially observed in semiconducting tunnel diodes<sup>[5]</sup> and was connected with the creation of definite phonons compensating for the large change of the electron momentum upon tunneling from the n region into the p region. The inelastic tunnel effect with emission of phonons was also observed recently in junctions between normal metals<sup>[6]</sup> and semimetals.<sup>[7]</sup> The substances investigated by the method of the inelastic tunnel effect are not limited to superconductors, and include also nonsuperconducting metals, semimetals, and semiconductors. In addition, information can be obtained concerning the spectral distribution of the phonon excitations in oxides and other inorganic compounds forming a barrier layer.<sup>[8]</sup> Particular interest attaches to a study of the vibrational excitations of impurity organic molecules adsorbed on an oxide layer.<sup>[9]</sup> The energies corresponding to such excitations lie in the interval from 0.1 to 0.5 eV. In addition, there is an obvious possibility of investigating magnon spectra in magnetically-ordered substances placed in a tunnel barrier, but no tunnel spectra of magnons have yet been observed experimentally.

In the present paper we report results of an investigation of tunnel spectra of phonons in Sn-Sn, Pb-Pb, and In-In junctions both in the normal and in the superconducting state, in the voltage interval from 0 to 150 mV. Corresponding to these voltages are excitations of the lattice vibrations of the metals forming the junction ( $V < 20$  mV), and excitations of oscillations of the lattices of the oxides ( $V < 100$  mV). The results of the investigation of the tunnel spectra of impurity organic molecules in these junctions are reported in<sup>[10]</sup>.

As seen from Figs. 1a and b, the final states of the

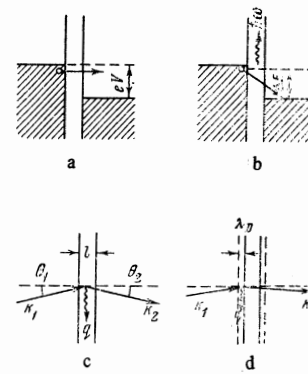


FIG. 1

electrons in elastic and inelastic tunneling are different, and their energies differ by an amount equal to the energy  $\Delta E = \hbar\omega$  of the excitation produced in the barrier. Thus, the inelastic tunnel process serves, as it were, as an additional channel for the penetration of the electrons through the potential barrier. It is clear that this channel becomes open only if the change of the electron energy following the tunnel transition is sufficient to produce the excitation. Therefore, with increasing voltage on the contact, more and more excitations, corresponding to ever-increasing energies, take part in the inelastic tunnel process. This is manifest in the junction characteristics by an increase of the conductivity which is faster the larger the number of excitations participating in the inelastic tunneling. From the general theory of inelastic tunnel processes<sup>[11,12]</sup> we obtain the following expression for the second derivative of the current-voltage characteristic:

$$\frac{d^2I^{(1)}}{dV^2} = \left(\frac{dI}{dV}\right)^0 \sum_q |\alpha(\mathbf{q}) \epsilon_q|^2 D_q(eV), \quad (1)$$

where  $(dI/dV)^0$  is the conductivity of the junction without allowance for the inelastic processes and  $D_q(eV)$  is the density of states for the excitations in the barrier. From (1) it follows that  $d^2I/dV^2$  is proportional to the spectral density of the excitations with energy  $eV$ , averaged over the momenta  $\mathbf{q}$  with a weight determined by the "form factor" of the creation of the excitation with momentum  $\mathbf{q}$  and polarization  $\epsilon_q$ . Thus, for phonon excitations the  $d^2I/dV^2$  characteristic is proportional to the density of

states of the phonons created in the barrier layer, and by "tunnel spectra" we mean in this entire paper the dependence of  $d^2I/dV^2$  on  $V$ .

The inelastic tunnel effect is a unique modification of absorption spectroscopy of substances either inside or in the immediate vicinity of the barrier. The spectral "probe" is the step of the Fermi distribution for the electrons in normal metals, which is smeared out in proportion to the absolute temperature. This smearing leads to a limitation of the resolution of the method, which amounts to approximately 6 kT.<sup>[9]</sup> Since the transition of a metal into the superconducting state is accompanied by the appearance of a sharp singularity in the dependence of the density of the electron states on the energy, connected with the occurrence of the energy gap  $2\Delta$  in the spectrum:  $\rho_S = \rho_N E / (E^2 - \Delta^2)^{1/2}$ , it follows that the resolution of the method increases greatly and, as a rule, is limited only by the sensitivity of the measuring apparatus. When metallic films become superconducting, all the absorption bands in the tunnel spectrum shift towards higher energies by an amount  $2\Delta/e$ , corresponding to the energy of breaking the Cooper pair. Therefore for all the spectra given below the abscissas used in the case of the superconducting states of films represent not the junction voltage  $V$ , but the quantity  $V' = V - 2\Delta/e$ .

## II. EXPERIMENTAL PROCEDURE

The tunnel junctions were prepared by the usual procedure,<sup>[13]</sup> but to obtain satisfactory tunnel characteristics some of the sputtering and oxidation parameters had to be chosen separately for each metal. All the films were condensed on a cooled substrate. The condensation temperature for tin films was 200°K, for lead 210°K, and for indium 160°K. When the tunnel junctions were heated to room temperature, a step necessary to mount the junctions in the cryostat, the tunnel resistance as a function of the temperature passed through a distinct maximum, the presence of which was a sufficiently reliable index of good quality of the sample.<sup>[13]</sup> The condensation rate in most cases was on the order of 10 Å/sec, and the dimensions of the tunnel junctions were  $1.0 \times 0.35$  mm. The resistances of the tunnel junctions ranged from 0.3 to 1000 ohms.

To obtain thin layers of oxide, the tin films were oxidized at room temperature in oxygen or air (ordinary or desiccated) at a pressure from 10 Torr to atmospheric. The oxidation time was 30 minutes. Lead films were oxidized in ordinary (nondesiccated) air at atmospheric pressure, and indium films in oxygen or desiccated air at a pressure not higher than 10–20 Torr. It should be noted that the difficulties in obtaining good tunnel junctions increase on going from Sn to Pb and In, and this correlates with such characteristics of the corresponding oxides as the energy of breaking the Me-O chemical bond or the heat of evaporation, which decrease in the series of oxides SnO<sub>2</sub>, PbO, and InO.<sup>[14]</sup> It is interesting that it is completely impossible to prepare In-InO-In tunnel junctions by the usual methods,<sup>[15]</sup> whereas we obtained Sn-SnO<sub>2</sub>-Sn and Pb-PbO-Pb junctions at relatively low resistivity ( $\rho_N < 1$  ohm-mm<sup>2</sup>), in spite of the fact that the Sn and Pb films are oxidized as a rule in an oxygen atmosphere at a temperature below 100°C.<sup>[16]</sup>

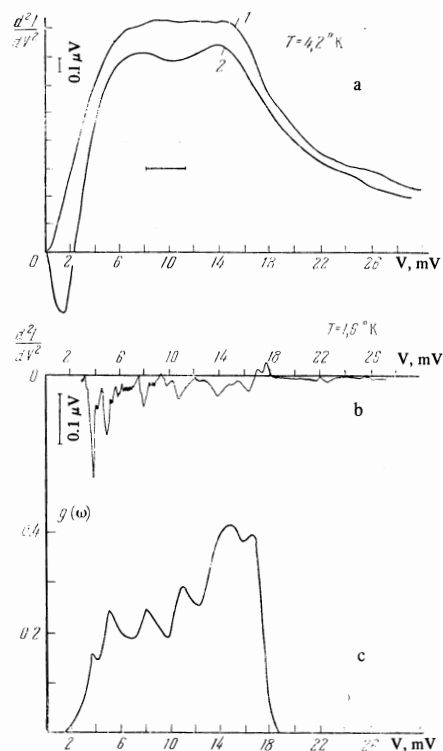


FIG. 2. a—Tunnel spectrum of the phonons of tin in Sn-SnO<sub>2</sub>-Sn junctions in the normal state. Junction resistances  $R_N$ : 1–9.5 ohms, 2–3 ohms. b—Phonon singularities of the density of the electron states in superconducting tin. Sn-SnO<sub>2</sub>-Sn junction,  $2V_1 = 300$   $\mu$ V. c—The function  $g(\omega) = \alpha^2(\omega)F(\omega)$ , where  $F(\omega)$  is the density of the phonon states for tin<sup>[17]</sup>.

The measuring system used to record the second derivative of the current-voltage characteristic had a sensitivity  $\sim 10^{-8}$  V in the channel of the second harmonic of the modulating signal. (The corresponding scale is designated by the vertical segment near the ordinate axis of Fig. 2.) The real sensitivity of the apparatus can be estimated from a comparison of the  $d^2I/dV^2$  characteristic for the Sn-Sn junction in the superconducting state (Fig. 2b) with the analogous curves that are well known from the literature.<sup>[16,17]</sup> The intensity of the spectral bands of the tunnel spectra can readily be obtained in units of  $mV^{-1}$ , which are convenient for a comparison of the characteristics of different junctions by using quantities directly measured in the experiment: the amplitude of the second-harmonic signal  $V_2$  (mV), the amplitude of the modulating signal  $V_1$  (mV), and the conductivity of the junction  $G_0$  at  $V = 0$ . Since the changes of the differential conductivity  $dI/dV$  do not exceed several percent in the investigated voltage interval, it follows that

$$\frac{dG}{dV} \approx 4 \frac{V_2}{V_1}, \quad G(V) = \frac{(dI/dV) - G_0}{G_0}. \quad (2)$$

The modulation frequency was 507 Hz. The amplitude of the modulating signal was chosen in accordance with the required resolution and the sensitivity of the measuring system and ranged from fractions of a millivolt to several millivolts. Usually the tunnel spectra were plotted at different levels of the modulating signal. Large amplitudes  $V_1$  revealed clearly the general contours of the absorption bands (Figs. 4 and 6–8), whereas the use

of small amplitudes of the modulating signal made it possible to veal the fine structure inside these bands (Figs. 5 and 9).

The quality of the tunnel junctions was verified by the shapes of the current-voltage characteristics in the superconducting state at voltages  $0 < V < 2\Delta/e$  and also by the  $d^2I/dV^2$  characteristics as functions of  $V$  in the region of voltages  $2\Delta/e < V < \Theta_D/e$ , analogous to the curve shown in Fig. 2b for Sn-SnO<sub>2</sub>-Sn junction. The level of additional current not of tunnel origin did not exceed several percent.

### III. EXPERIMENTAL RESULTS

#### 1. Tunnel Spectra of Sn-SnO<sub>2</sub>-Sn Junctions

Figures 2 and 4-7 show the tunnel spectra of Sn-SnO<sub>2</sub>-Sn junctions. The doubled amplitude of the modulating voltage is designated in the form of a horizontal segment located near the corresponding curves. The null of the ordinate scale is shifted arbitrarily for convenience in comparison of the different curves, with the exception of those cases when the position of the null on the ordinate axis is specially indicated.

The broad band for  $0 < V < 18$  mV at  $T > T_C(\text{Sn})$  is obviously due to the tunnel effect with emission of phonons in the tin films and reflects the dependence of the density of states of the phonons participating in the inelastic tunneling on the energy  $\hbar\omega = eV$ . By comparing this dependence with the function  $g(\omega) = \alpha^2(\omega) F(\omega)$  plotted by reducing the  $d^2I/dV^2$  characteristics of the Sn-Sn junctions in the superconducting state<sup>[17]</sup> (Fig. 2c), we note that the width of the band corresponds to the width of the spectrum of the phonons in tin (end-point energy 18 meV), but the distribution of the density of states with respect to the energies differs from the  $g(\omega)$  curve corresponding to the bulky metal. The density of states of the phonons participating in the inelastic tunnel effect has as a rule two maxima at  $\sim 7$  and  $\sim 14$  mV (curve 2 on Fig. 2a). For some junctions, these maxima are not resolved (curve 1 on Fig. 2a). The complex structure of the phonon spectrum  $g(\omega)$ , which is well marked on the  $d^2I/dV^2$  characteristics of these junctions in the superconducting state (Fig. 2b), is not observed on the inelastic-tunnel-effect characteristics even when  $V_1$  is decreased to 1 mV. At a voltage of approximately 1.5 mV, a minimum of  $d^2I/dV^2$  as a function of  $V$  is observed for certain junctions (curve 2 on Fig. 2a), corresponding to a maximum of  $dI/dV$  at  $V = 0$ , with a width on the order of several mV. This singularity, called in the literature<sup>[18]</sup> the "zero anomaly," is due to the scattering of electrons by paramagnetic impurities in the barrier and is not considered in the present paper. The tunnel effect itself with emission of phonons leads to the occurrence of a minimum of  $dI/dV$  at  $V = 0$  (Fig. 3). The width of the minimum with respect to voltage is  $eV \sim \Theta_D$ , and the depth is  $\sim 4\%$  of the "background" conductivity at  $V = 0$ . Figure 3 also shows clearly the stepwise increase of the conductivity of the junction at voltages  $V \approx 0.18$  V and  $V \approx 0.36$  V, due to excitation of molecular impurities in the barrier. The minimum of the background conductivity is shifted to the left by 0.1 V, something already noted by Rowell for Al-Al<sub>2</sub>O<sub>3</sub>-Sn junctions.<sup>[6]</sup> In addition, the dependence of  $dI/dV$  on  $V$  has a noticeable asymmetry. At positive  $V$ , the background con-

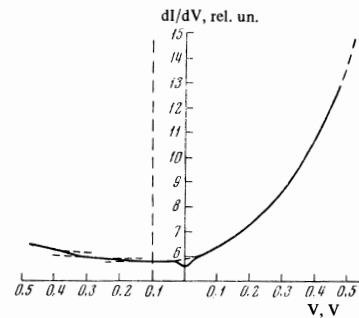


FIG. 3. Dependence of the conductivity of the Sn-Sn junction on the voltage (solid curve)  $T = 4.2^\circ\text{K}$ ,  $R_N = 16$  ohm, the dashed lines approximate the proposed course of the phonon conductivity near  $V = 0$  and also at  $V = 0.18$  and  $0.36$  V. The vertical dashed line crosses the experimental curve at the point of the minimum of the phonon conductivity.

ductivity increases much faster than at negative ones. (Negative  $V$  correspond to negative polarity of the lower, oxidized film.) However, the intensities of the bands in the tunnel spectra discussed below are symmetrical, within the limits of the scatter of the experimental data relative to the ordinate axis ( $\sim 10\%$ ), with respect to reversal of the sign of the applied voltage, although the rapidly increasing background of  $dI/dV$  makes their observation at  $V > 0$  less convenient.

At voltages near 45 mV there begins a new band of the tunnel spectrum, terminating at  $V \sim 100$  mV. The intensity of this band is smaller by approximately one order of magnitude than that of the preceding one, and to observe it clearly it is necessary to increase the amplitude of the modulating signal. Figures 4, 6, and 7 show clearly the general contours of these bands, whereas Fig. 5 shows the structure of the spectrum inside the band, revealed when the modulating-signal level is lowered. This band is obviously due to excitation of the optical phonons in the tin oxide. This point of view is confirmed by comparing the published data<sup>[19]</sup> on the absorption bands of SnO<sub>2</sub> in the IR spectrum with the results of tunnel measurements. The energies of the optical phonons participating in the absorption of IR radiation are<sup>[19]</sup> 54.5-59.3, 77.3, and 96.5 mV. These energies fall inside the considered 45-100 mV band in the tunnel spectra of the Sn-SnO<sub>2</sub>-Sn junctions (Figs. 3, 5, 6). We have attempted to observe the fine structure inside this band, working with the minimum possible levels of the modulating signal ( $2V_1 \approx 5$  mV).

Figure 5 shows the tunnel spectra of the optical phonons in tin oxide for six different samples. The resistances of the Sn-Pb junctions are respectively 2.1, 4.6, and 65 ohms (curves 1, 2, 3), and the resistances of the Sn-Sn junctions are 2.55, 19.5, and 28 ohms (curves 4, 5, 6). It can be seen that within the indicated limits of variation of the tunnel resistances, the form of the spectrum remains the same in general outline. The difference between the envelope contour of this band for the Sn-Sn junctions and the Sn-Pb junctions is to a considerable degree illusory. It is due to a strong background signal that decreases with increasing voltage and is present in the Sn-Sn junctions but is appreciably attenuated in the Sn-Pb junctions. The source of this signal is connected with the "tail" of the last phonon singularity in the density of the electron states of the super-

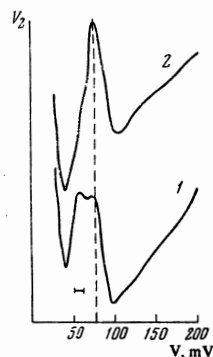


FIG. 4. Different forms of the band of the optical phonons of the Sn oxide. Curve 1— $R_N = 166$  ohms, 2— $R_N = 220$  ohms.

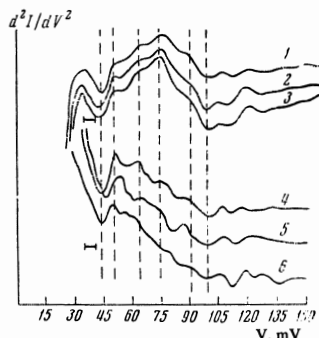


FIG. 5. Structure of the band of the optical phonons of the Sn oxide. 1, 2, 3, 6— $T = 4.2^\circ\text{K}$ ; 4, 5— $T = 1.6^\circ\text{K}$ ; 1–3—Sn-Pb junctions, 4–6—Sn-Sn junctions.

conducting Sn (Fig. 2b), which is greatly enlarged by large values of  $V_1$ . It must be emphasized that the discussed band in the tunnel spectrum of the oxide ( $V = 45$ – $100$  mV) is not connected with the superconductivity of Sn and is observed both at  $T > T_c$  and at  $T < T_c$ .

The spectra of Fig. 5 show clearly the fine structure which, unfortunately, cannot be uniquely related at present with the Sn oxide only. Indeed, an analogous structure extends also into the region of larger  $V$ , where, as is well known, are located the absorption bands of the organic impurity molecules.<sup>[9,10]</sup> An experimental study of the tunnel spectra of low-resistance ( $R_N < 30$  ohm) Sn-SnO<sub>2</sub>-Sn and Sn-SnO<sub>2</sub>-Pb junctions up to voltages  $\sim 0.5$  V (Fig. 6) convinces us of the presence of such impurities in the barrier. Figure 6 shows clearly the spectral bands ( $V = 0.18$  V,  $0.36$  V) due to organic impurities that fall in the barrier upon oxidation of the lower Sn film in ordinary air (curves b and c), which coincide well with the data of Lamb and Jaklevic for Al-Al<sub>2</sub>O<sub>3</sub>-Pb junctions (curve a).

With increasing junction resistance ( $R_N > 100$  ohms), the absorption bands of the impurity molecules vanish (Fig. 4). This is probably connected with the attenuation of the adsorption forces with increasing oxide thickness, which leads to almost complete desorption of the impurity molecules in the vacuum after the oxidation.<sup>[20]</sup> All that remains on the spectrum is the band at  $V = 45$ – $100$  mV (curves 1 and 2 of Fig. 4), the shape of which changes noticeably with increasing oxide thickness. The observed change of the contours of the band is obviously connected with changes in the structure of the oxide. Possibly, a transition takes place from processes of coherent excitation of the phonons to incoherent inelastic processes, in which connection changes take place also in the selection rules.<sup>[12]</sup> Curve 1 of Fig. 4 shows, as before, a certain structure of the oxide

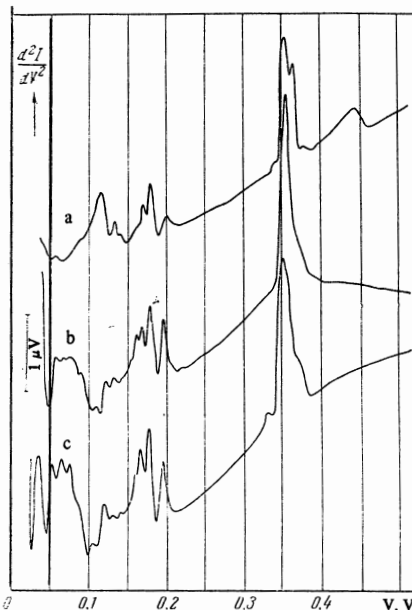


FIG. 6. a—Tunnel spectrum of Al-Al<sub>2</sub>O<sub>3</sub>-Pb junctions according to the data of Lamb and Jaklevic<sup>[9]</sup>; b—tunnel spectrum of Sn-SnO<sub>2</sub>-Sn junctions; c—the same for Sn-SnO<sub>2</sub>-Pb.  $T = 1.6^\circ\text{K}$ ,  $2V_1 = 8$  mV.

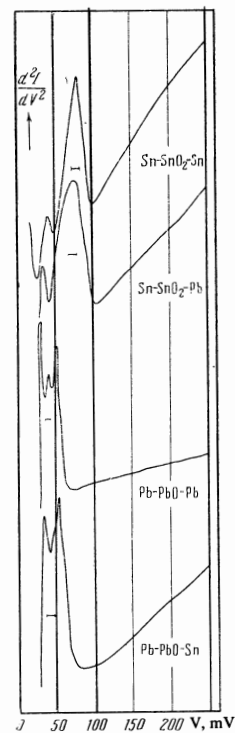


FIG. 7. Comparison of the tunnel spectra of tin and lead junctions. Sn-Sn junction resistance 750 ohms.

band, but its detailed investigation at low levels of the modulating signal turned out to be impossible, since the effective sensitivity of the measuring apparatus decreases with increasing sample resistance. Thus, the question of the origin of the fine structure in the region  $V = 45$ – $100$  mV must remain open for the time being.

It is possible to verify directly the correctness of connecting the broad band  $V = 45$ – $100$  mV with the excitations of the tin oxide by comparing the tunnel spectra for Sn-SnO<sub>2</sub>-Sn, Sn-SnO<sub>2</sub>-Pb, Pb-PbO-Sn, and Pb-PbO-Pb junctions containing no impurity molecules, as

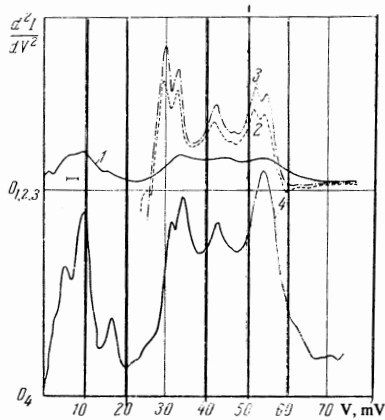


FIG. 8. Tunnel spectra of Pb-PbO-Pb junction, obtained at different temperatures: 1—8°K, 2—4.2°K, 3—1.5°K, 4—1°K [6].

is evidenced by the absence of absorption bands in the region  $V = 100\text{--}250$  mV (Fig. 7). The spectral band at  $V = 45\text{--}100$  mV is observed in Sn-Sn and Sn-Pb junctions with a barrier of  $\text{SnO}_2$ . In Pb-Pb and Pb-Sn junctions with a barrier of PbO there is observed a band whose characteristics will be described in detail in the next section. By comparing the spectra of the Sn-Pb and Pb-Sn junctions we can readily see that in spite of the fact that the materials of the electrodes coincide in both cases (Sn, Pb), a change in the barrier material ( $\text{SnO}_2 \rightarrow \text{PbO}$ ) actually leads to the expected change of the spectrum.

## 2. Tunnel Spectra of Pb-PbO-Pb Junctions

The tunnel spectra of the Pb-PbO-Pb junctions were investigated experimentally most thoroughly, making it possible to compare our data with the results by others.<sup>[6]</sup> Figure 8 shows the tunnel spectra obtained at different temperatures. Curves 1, 2, and 3 correspond to the temperatures 8, 4.2, and 1.5°K, with the lead in the superconducting state at  $T = 4.2$  and 1.5°K; we therefore do not present the section of the spectrum at voltages smaller than 25 mV for curves 2 and 3. Its form corresponds fully to the known published<sup>[16]</sup>  $d^2I/dV^2$  characteristics. Curve 4 corresponds to the data of Rowell<sup>[6]</sup> for the tunnel spectrum of the Pb-Pb junction in the normal state at  $T = 1^\circ\text{K}$ . The superconductivity of lead was destroyed by a magnetic field. It is seen from Fig. 8 that all the curves correlate well with one another.

The band at voltages  $V < 10$  mV in the tunnel spectrum is due to excitation of the phonons in the Pb films, whereas the band at 25–65 mV is obviously connected with optical phonons in the lead oxide. The two peaks in the tunnel spectrum at 10 and 6 mV can be set in correspondence with the characteristics of the longitudinal (8.8 mV) and transverse (4.5 mV) phonons in lead. The peak at  $\sim 17$  mV is apparently connected either with multiphonon processes in the metallic films or with the phonons in the Pb oxide.

A striking agreement in almost all details is revealed by the spectrum of the optical phonons of lead oxide, which has a complicated structure. We recall that in Rowell's investigation<sup>[6,16]</sup> the procedure of producing the junctions differed from that de-

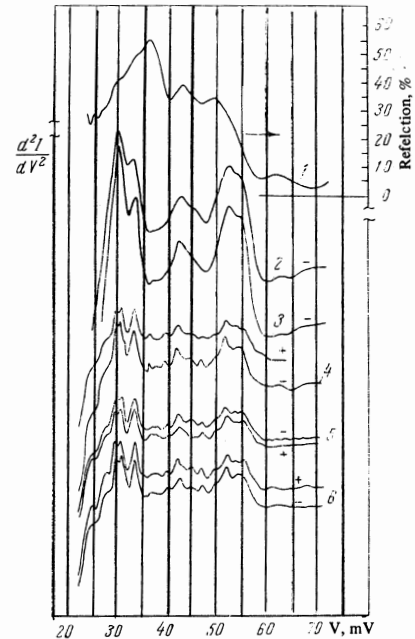


FIG. 9. Lead-oxide spectra: 1—IR reflection spectrum of PbO. 2—6—tunnel spectra.  $V_1 = 1.5$  mV for curves 2 and 3,  $V_1 = 0.5$  mV for curves 4–6, where the ordinate scale is increased by a factor of 3.  $R_N(2, 5) = 5.6$  ohms,  $R_N(3, 4, 6) = 2.9$  ohms.

scribed in Sec. 2, namely the films were condensed on a substrate at room temperature, and the oxidation was in oxygen at a temperature of  $\sim 50^\circ\text{C}$ . Nonetheless, the spectra of the optical phonons of the oxide differ only in minor details from each other, thus indicating the stability of the composition and structure of the PbO oxide film. The simplest oxide of lead is PbO, which exists in two crystal modifications: orthorhombic (yellow) and tetragonal (red).<sup>[14]</sup>

We have made a direct comparison of the tunnel spectra of the lead oxide with the IR reflection spectrum from a PbO layer of the yellow modification, obtained by condensation of lead monoxide in vacuum on a glass substrate at room temperature. We also plotted the transmission spectrum of PbO. In this case the substance was condensed on a substrate of single-crystal CsI. Both IR spectra were well correlated with each other. The result of the comparison is shown in Fig. 9, where curve 1 gives the IR reflection spectrum of PbO, and curves 2 and 3 give the tunnel spectra for two different Pb-PbO-Pb junctions. The tunnel spectra were well reproduced in different samples and, as can be seen from Fig. 9, were similar in shape to the IR spectrum. Indeed, the beginning and the end of the spectrum of the optical phonons as obtained from the IR and tunnel diode coincide. Moreover, both the infrared and the tunnel spectra have three broad bands which approximately coincide in energy. Such a qualitative agreement between the spectra makes it possible to relate the observed band in the tunnel spectrum uniquely to excitations of optical phonons in the lead oxide, and also to advance the hypothesis that the composition of the oxide film is close to PbO. In addition, the complex structure of the tunnel spectrum obviously points to the existence of long-range order in the oxide, and consequently indicates a sufficiently perfect structure of the oxide film

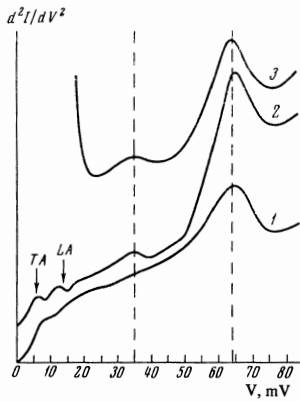


FIG. 10. Tunnel spectra of In-InO-In junction. Curve 1—prior to annealing,  $V_1 = 2$  mV,  $R_N = 3$  ohm,  $T = 4.2^\circ\text{K}$ ; 2—after annealing at room temperature for one day,  $V_1 = 2$  mV,  $R_N = 1.41$  ohm,  $T = 4.2^\circ\text{K}$ ; 3— $T = 1.6^\circ\text{K}$ . For curves 2 and 3, the vertical scale is stretched out by a factor of three compared with curve 1.

in the plane of the junction, and its homogeneity in thickness. The latter is also confirmed by the results of a study, for the same junctions, of the oscillatory dependence of the critical Josephson current on the magnetic field, which is strongly influenced by the most minute thickness inhomogeneities of the oxide layer.<sup>[21]</sup>

The decrease of the amplitude of the modulating voltage  $V_1$ , accompanied by an increase of the resolution, leads to the appearance of a fine structure of the band of the optical phonons, which was not noted in earlier investigations.<sup>[6,18]</sup> This structure is also satisfactorily duplicated for different samples (curves 4–6 in Fig. 9). In Fig. 9, curves 2 and 5, and also 3 and 6, pertain to the same samples, and the signs next to the curves indicate the polarity of the lower oxidized film. It is difficult at present to interpret the observed spectrum, but it can be assumed that a definite role may be played by effects of size quantization in a direction perpendicular to the plane of the junction, or else by multiphonon processes. The spectra of the Pb-PbO-Pb junctions never revealed any absorption bands of impurity organic molecules at  $V = 100$ – $500$  mV,<sup>[10]</sup> making it possible to attribute the observed fine structure of the 25–60 mV band to oscillations of the lead oxide.

### 3. Tunnel Spectra of In-InO-In Junctions

Figure 10 shows the tunnel spectra of In-InO-In junctions, on which one can see spikes due both to phonons in the metallic films (TA—transverse and LA—longitudinal), as well as to phonons in the oxide ( $V = 35$  mV and  $V = 64$  mV). The main feature of the spectra of indium junctions consists of a low intensity of the phonon emission in the metallic films. In addition, the spectrum of the oxide phonons consists of only two smeared bands, which apparently indicate that the oxide has a disordered structure. Qualitatively, analogous spectra of optical phonons were obtained by Giaever<sup>[8]</sup> for substances (CdS, ZnS) introduced artificially into the interior of the tunnel junction. Obviously, the structure of the dielectric films obtained in this manner is also quite imperfect.

The In films have the property, noted already by Rowell,<sup>[16]</sup> that in order to obtain distinct phonon singularities on the superconducting tunnel characteristics they must be annealed at room temperature. This effect was observed by us both for phonon singularities manifest in the density of the electron states in the superconducting indium, and on the characteristics of inelastic tunneling (curves 1 and 2 in Fig. 10). In the latter

case, however, the magnitude of the effect is not so appreciable. We note that just as for the Pb-PbO-Pb junctions, no absorption bands of the impurity organic molecules were observed in the In-InO-In junctions.

## IV. DISCUSSION OF EXPERIMENTAL RESULTS

### 1. Selection Rules

The interpretation of the experimental results depends essentially on the selection rules determined by the dependence of the form factor  $|\alpha(\mathbf{q}) \epsilon_{\mathbf{q}}|^2$  in expression (1) on the quasimomentum  $\mathbf{q}$  and on the polarization  $\epsilon_{\mathbf{q}}$  of the produced excitations. In the inelastic tunnel process it is necessary to satisfy the energy conservation law

$$E(\mathbf{k}_1) = E(\mathbf{k}_2) + \hbar\omega_{\mathbf{q}}. \quad (3)$$

In addition, if the excitation of the quasiparticles in the barrier is coherent, then the momentum component tangential to the barrier should also be conserved:

$$k_1^{\parallel} = k_2^{\parallel} + q^{\parallel}. \quad (4)$$

The conservation law for the parallel component of the quasimomentum is satisfied only if the system is homogeneous in directions tangent to the barrier, i.e., the barrier does not contain random scattering centers, and the reflection of the electrons from the boundaries between the metal and the oxide is specular.

Let us consider first the excitation of optical phonons propagating in the oxide along the barrier (Fig. 1c). The effective interaction of the electron with the oxide lattice will be observed only for electrons traveling at small angles  $\theta_1$  and  $\theta_2$  to the barrier, since the only electrons penetrating deep into the barrier are those moving almost perpendicular to the surface of the junction. Consequently, optical phonons with small  $q^{\parallel}$  will be produced in the main. The polarization of such phonons should be transverse for maximum interaction with the tunneling electrons. It is interesting that these selection rules are similar to the corresponding rules in IR spectroscopy. It is possible that this explains the similarity of the spectra, which was noted in the discussion of Fig. 9.

In the same model with specular boundaries for the optical phonons propagating perpendicular to the barrier along the  $z$  axis, standing waves should arise and the allowed values of  $q_z$  correspond to the quantum size effect for phonons in an oxide layer of thickness  $l$ :

$$q_z = n \frac{\pi}{l} \ll q_D, \quad n = 1, 2, 3, \dots \quad (5)$$

For effective interaction with the tunneling electron, such phonons should have a longitudinal polarization. Since the barrier thickness is small and contains not more than several molecular layers ( $l = ma$ , where  $m = 3$ – $4$  and  $a$  is the oxide lattice parameter), the spectrum should consist of 3–4 bands, the distance between which should depend significantly on the thickness of the oxide layer (and consequently on the junction resistance). We have investigated in detail the spectrum of the phonons of lead oxide, the form of which corresponded to curves 2 and 3 in Fig. 6, for junctions whose resistances differed by more than 20 times. If the observed bands were to be connected with the size quantization, then calculation would predict a shift of their positions on the

voltage axis by an amount  $\sim 10\%$ . In actual fact, no shift of the bands was observed in the experiment, within the limits of experimental error, the latter being  $\sim 1\%$ . Consequently, this can also serve as indirect confirmation that the observed spectrum is connected with optical phonons propagating along the oxide layer. We were unable to trace the dependence of the position of the singularities of the fine structure of the band of optical phonons of PbO, owing to the insufficient sensitivity of the measuring apparatus.

For the phonons produced in the metallic films (Fig. 1d), a similar situation arises. In order to be able to consider the tunneling process and the phonon-emission process as simultaneous, it must be assumed that the phonons are produced in a narrow layer of metal near the boundary with the oxide. In this layer, the width of which is of the order of  $\lambda_D = [4\pi e^2 N(\epsilon_F)]^{-1/2}$ , the barrier potential overlaps the metal-lattice potential, i.e., the surface layer of the metal is part of the potential barrier, and the metal-lattice vibrations are only partly screened by the conduction electrons, leading to noticeable oscillations of the barrier potential. Thus we conclude that surface phonons, the spectrum of which differs from the spectrum of the phonons in a bulky sample, are apparently in metallic films.

If the barrier contains a large number of scattering centers, then the law of conservation of the parallel component of the quasimomentum (4) will not hold.<sup>[12]</sup> There should be observed in the spectrum an intense line corresponding to longitudinal optical phonons with  $q = 0$ , and a singularity of lower intensity, located at lower energies and corresponding to the transverse optical phonons. We can interpret in this manner the observed tunnel spectra of indium oxide (Fig. 10) and tin oxide for high-resistance junctions (curve 1 on Fig. 4 and on Fig. 7).

## 2. Intensity of Absorption Bands

On the basis of the advanced considerations, we can attempt to understand certain regularities observed in the experiments. The greatest peak heights due to the phonons in the metallic films are observed for Sn-Sn contacts ( $152 \pm 8$  relative units proportional to  $dG/dV$ ). It can be assumed that this is connected, on the one hand, with the existence of optical phonons in this metal and, on the other hand, with the relatively low symmetry of the Fermi surface. It follows from the phonon spectrum of  $\beta$ -Sn<sup>[22]</sup> that the density of states of the transverse optical phonons is maximal in the energy intervals 5–6 and 13–16 MeV, which is in satisfactory agreement with the singularities of the tunnel spectrum. The low symmetry of the Fermi surface in  $k$ -space leads apparently to a larger relative weight of the inelastic tunnel processes accompanied by a change of  $k^{\parallel}$ . From this point of view we can also understand the relatively lower height of the phonon peak for Pb ( $87 \pm 11$  relative units), in spite of the fact that the electron-phonon interaction in this metal is stronger than in Sn. Moreover, in Sn-Pb contacts at  $T > T_C(\text{Pb})$  the phonon spectrum at voltages  $V = 0\text{--}45$  mV was a reflection of phonon production in the tin film, i.e., it was similar to the spectrum for the Sn-Sn junctions. The relative height of the peak, as expected, was lower than for the Sn-Sn junctions, and

amounted to 80–90 relative units. The height of the phonon peak has the lowest value in indium junctions (Fig. 10).

The height of the peaks due to excitation of phonons in oxides is maximal for PbO and minimal for SnO<sub>2</sub>.

## 3. Parameters of Effective Potential Barrier

In the simple model of a symmetrical potential barrier with effective height  $\bar{\varphi}$  and width  $s$ , the dependence of the conductivity of the junction on the voltage should be described by a parabola<sup>[18]</sup> that is symmetrical with respect to the ordinate axis. The real  $dI/dV$  curves, as a rule, are not symmetrical and are shifted along the abscissa by an amount 0.1–0.2 V<sup>[6,18]</sup> (Fig. 3). Nonetheless, taking this shift into account, we attempted to plot  $dI/dV$  against  $V$  for different junctions in the voltage interval from 0 to  $\pm 0.5\text{--}1.0$  V and to determine the effective barrier parameters from these curves. The effective barrier height  $\bar{\varphi}$  obtained in this manner corresponds approximately to half the width of the forbidden band in the oxide,  $\bar{\varphi} = E_g/2$ , making it possible to determine this parameter for all the oxides investigated by us. For SnO<sub>2</sub>, PbO, and InO we obtain for  $E_g$  the respective values 3.6–4.1, 2.6–2.8, and 3.8 eV, in satisfactory agreement with the handbook data: 3.5 eV for SnO<sub>2</sub> and 2.54 eV for PbO ( $E_g = 1.49$  eV for PbO<sub>2</sub>).

Starting from the same model, we obtain for most junctions an effective barrier width  $s \approx 13\text{--}15 \text{ \AA}$ .

In conclusion we emphasize that inelastic tunnel spectroscopy makes it possible to investigate the structure of the oxide directly inside the tunnel junction, an important factor, for example, for the choice of various selection rules in tunneling from single crystals.<sup>[23]</sup> From the obtained spectra of the oxides (Figs. 3–9) we conclude that thin films of Pb oxide have a sufficiently perfect structure, and films of thin oxide at small thicknesses are sufficiently perfect, but at large thicknesses they are almost amorphous, with large numbers of scattering centers. Finally, films of indium oxides are almost amorphous even at relatively small thicknesses ( $R_N \leq 3$  ohms) or else contain a large number of scattering centers.

I am deeply grateful to V. Kut'ko for IR spectroscopy of the lead oxide and to A. Maksimov for help with preparing the samples.

<sup>1</sup>I. Giaever and K. Megerle, Phys. Rev. **122**, 1101 (1961).

<sup>2</sup>N. V. Zavaritskiĭ, Zh. Eksp. Teor. Fiz. **45**, 1839 (1963); **48**, 837 (1961) [Sov. Phys.-JETP **18**, 1260 (1964); **21**, 557 (1965)].

<sup>3</sup>L. Esaki and P. Stiles, Phys. Rev. Lett. **14**, 902 (1965).

<sup>4</sup>P. Gray, Phys. Rev. **140**, A179 (1965).

<sup>5</sup>N. Holonyak, I. A. Lesk, R. N. Hall, J. J. Tiemann, and H. Ehrenreich, Phys. Rev. Lett. **3**, 167 (1959).

<sup>6</sup>J. M. Rowell, W. L. McMillan, and W. L. Feldmann, Phys. Rev. **180**, 658 (1969).

<sup>7</sup>L. Esaki, L. L. Chang, P. Stiles, D. O'Kane, and N. Wisner, Phys. Rev. **167**, 3k (1968).

<sup>8</sup>I. Giaever and H. R. Zeller, Phys. Rev. Lett. **21**, 1385 (1968).

- <sup>9</sup>J. Lambe and R. Jaklevic, *Phys. Rev.* **165**, 821 (1968).
- <sup>10</sup>I. K. Yanson and N. I. Bogatina, *Zh. Eksp. Teor. Fiz.* **59**, 1509 (1970) [*Sov. Phys.-JETP* **32**, 823 (1971)].
- <sup>11</sup>D. J. Scalapino, *Electron Tunneling as a Probe of Barrier Excitations*, Preprint, 1968.
- <sup>12</sup>A. J. Bennett, C. B. Duke, and S. D. Silverstein, *Phys. Rev.* **176**, 969 (1968).
- <sup>13</sup>I. O. Kulik and I. K. Yanson, *Éffekt Dzhozefsona v sverkhprovodyashchikh tunnel'nykh strukturakh* (Josephson Effect in Superconducting Tunnel Structures), Nauka, 1970, pp. 146-161.
- <sup>14</sup>G. V. Samsonov et al., *Fiziko-khimicheskie svoïstva okislov, spravochnik* (Physicochemical Properties of Oxides. A Handbook), Metallurgiya, 1969, pp. 121, 154, 25, 288.
- <sup>15</sup>I. Giaever, in *Tunneling Phenomena in Solids*, Plenum Press, N. Y., 1969, p. 23.
- <sup>16</sup>J. Rowell and L. Kopf, *Phys. Rev.* **137**, 1907 (1965).
- <sup>17</sup>N. V. Zavaritskii, *Zh. Eksp. Teor. Fiz.* **57**, 752 (1969) [*Sov. Phys.-JETP* **30**, 412 (1970)].
- <sup>18</sup>J. M. Rowell, in *Tunneling Phenomena in Solids*, Plenum Press, N.Y., 1969, pp. 385-392.
- <sup>19</sup>J. R. Beattie, *J. Chem. Soc.*, 2322, (1969).
- <sup>20</sup>L. H. Little, *Infrared Spectra of Adsorbed Species*, Academic, 1967.
- <sup>21</sup>I. K. Yanson, *Zh. Eksp. Teor. Fiz.* **58**, 1497 (1970) [*Sov. Phys.-JETP* **31**, 800 (1970)].
- <sup>22</sup>E. G. Brovman and Yu. M. Kagan, *ibid.* **52**, 557 (1967) [**25**, 365 (1967)].
- <sup>23</sup>J. E. Dowman, M. MacVicar, and J. R. Waldram, *Phys. Rev.* **186**, 452 (1970).

Translated by J. G. Adashko  
193